Inorganic Chemistry

Article

pubs.acs.org/IC

Regulation of Aggregation Behavior and Neurotoxicity of Prion Neuropeptides by Platinum Complexes

Xuesong Wang,[†] Menghan Cui,[†] Cong Zhao,[†] Lei He,[†] Dengsen Zhu,[†] Baohuai Wang,[‡] and Weihong Du*[,†]

[†]Department of Chemistry, Renmin University of China, Beijing 100872, People's Republic of China

[‡]College of Chemistry and Molecular Engineering, Peking University, Beijing 100871, People's Republic of China

Supporting Information

ABSTRACT: Prion diseases belong to a group of infectious, fatal neurodegenerative disorders. The conformational conversion of a cellular prion protein (PrP^{C}) into an abnormal misfolded isoform (PrP^{Sc}) is the key event in prion disease pathology. PrP106−126 resembles PrP^{Sc} in some physicochemical and biological characteristics, such as apoptosis induction in neurons, fibrillar formation, and mediation of the conversion of native cellular PrP^{C} to PrP^{Sc}. Numerous studies have been conducted to explore the inhibiting methods on the aggregation and neurotoxicity of prion neuropeptide PrP106−126. We showed that PrP106−126 aggregation, as assessed by fluorescence assay and atomic force microscopy, is inhibited by platinum complexes cisplatin, carboplatin, and $Pt(bpy)Cl_2$. ESI-MS and NMR assessments of PrP106−126 and its mutant peptides demonstrate that platinum complexes bind to the peptides in coordination and nonbonded interactions, which rely on the ligand properties and the peptide sequence. In peptides, methionine residue is preferred as a potent binding site over histidine residue for the studied platinum complexes, implying a typical thiophile characteristic of platinum. The neurotoxicity induced by PrP106−126 is better inhibited by $Pt(bpy)Cl_2$ and cisplatin. Furthermore, the ligand configuration contributes to both the binding affinity and the inhibition of peptide aggregation. The pursuit of novel platinum candidates that selectively target prion neuropeptide is noteworthy for medicinal inorganic chemistry and chemical biology.

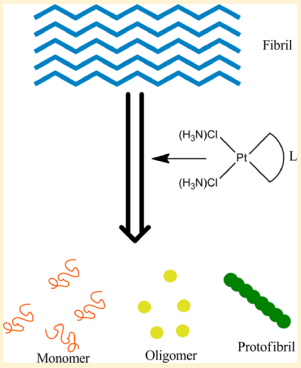

INTRODUCTION

Prions are transmissible particles that cause a group of invariably fatal neurodegenerative diseases, such as bovine spongiform encephalopathy and human Creutzfeldt−Jakob disease.[1] Prion propagation involves the conversion of cellular prion protein (PrP^{C}) into a disease-specific isomer, PrP^{Sc}, shifting from predominant α-helices to β-sheet structure.[2] Pathogenic mutations and modifications as well as some cofactors, such as glycosaminoglycans, nucleic acids, and lipids, could modulate the conformational conversion process.[3] The major conformational change that occurs during conversion of PrP^{C} into PrP^{Sc} has been localized to residues 90−112. Otherwise, residues 113−126 constitute the conserved hydrophobic region that also displays structural plasticity.[4] The structural transition of PrP^{C} to PrP^{Sc} is accompanied by profound changes in the physicochemical properties of PrP. PrP^{Sc} assembles into amyloid fibrils at slightly acidic or neutral pH, and the amyloid form displays a remarkable resistance to proteinase K.[5,6] The accumulation of PrP^{Sc} is also the most possible reason for cell death, inflammation, and spongiform degeneration observed in infected individuals.[7]

Human prion neuropeptide PrP106−126 is an N-terminal segment of the full length prion protein that resembles PrP^{Sc} in ways such as induction of apoptosis in neurons, fibrillar formation, resistance to protease K digestion, and mediation of the conversion of PrP^{C} to PrP^{Sc}.[8−10] Although it is impossible for the short peptide PrP106−126 to represent PrP^{Sc} completely, it is a common research model to investigate neurodegeneration in prion diseases because it encompasses the core structure and hydrophobic region of prion protein.[11−14] Other prion peptides such as PrP118−135 and PrP185−208 have been employed to study their basic physicochemical properties associated with neurotoxicity and aggregation.[15,16] PrP118−135, which is highly conserved among various species and shares homology with the C-terminal domain of the Alzheimer's β-amyloid peptide (Aβ), can form amyloid fibrils and induce liposome fusion in a nonaggregated form via an apoptotic pathway.[17] PrP185−206 can also cause the destabilization of the membrane, making it permeable to potassium ion and charged organic compounds.[18]

In PrP106−126, the spanning fragment of Asn108−Met109−Lys110−His111−Met112 presents a "turn-like" conformation with the His111 situated before the starting point of the α-helix. The effect of His111 is exerted by changes in its hydrophobicity, triggering aggregation of the peptide. The amphiphilic properties of His111 may thus be important for the modulation of the conformational mobility and heterogeneity of PrP106−126.[19] Methionine oxidation has been reported to significantly reduce amyloid fibril formation and proteinase K resistance, but it does not reduce the neurotoxicity of peptides in vivo and in vitro.[20,21] Chicken prion peptide 119−139 corresponds to that of human PrP106−126, except for the varieties of methionine 122 and 125, which could be regarded as a mutant of PrP106−126. Bovine

Received: January 14, 2014
Published: May 2, 2014

   dx.doi.org/10.1021/ic500092t | Inorg. Chem. 2014, 53, 5044−5054

prion peptide 109−129 resembles human PrP106−126 as well, except for the difference in methionine 115. The bovine PrP109−129, with Met112 alone, shows both reduced fibrosis capacity and neurotoxicity.[22−24] Taking into account all the above characteristics of residues Met109, His111, and Met112, six prion peptides with the three amino acids mutated were employed in our study (Table 1).

Table 1. Peptide Names, Sequences, and Abbreviations Used in This Study

peptide sequence	mutated site	abbreviation
KTNMKHMAGAAAAGAVVGGLG	none	PrP106−126
KTNMKAMAGAAAAGAVVGGLG	H111	H111A
KTNFKHVAGAAAAGAVVGGLG	M109, M112	M109F/M112 V
KTNMKAVAGAAAAG	H111, M112	H111A/M112 V
KTNFKHMAGAAAAG	M109	M109F
KTNFKAMAGAAAAG	M109, H111	M109F/H111A
KTNMKHVAGAAAAG	M112	M112 V

Some studies have reported the inhibition effect of PrP106−126 either on aggregation behavior or on neurotoxicity. For instance, small stress molecules inhibit the aggregation and neurotoxicity of PrP106−126 by preventing protein denaturation and maintaining protein stability.[25] Tetracycline and its derivatives may exert antifibrillogenic activity on PrP106−126,[26] and carnosine inhibits both the β-sheet formation and the neurotoxicity of PrP106−126.[27] Some transition-metal ions, such as Cu^{2+}, Zn^{2+}, Mn^{2+}, and Ni^{2+}, also reportedly bind with PrP106−126.[28−31] However, noble-metal complexes, including gold and palladium, could inhibit the aggregation and neurotoxicity of PrP106−126 and its mutant peptides.[32−35] Palladium complexes inhibit peptide aggregation through ligand-induced special effect more effectively than the binding interaction of complexes to PrP106−126.[33] Ruthenium complex has also been selected for its low cytotoxicity and better binding affinity to PrP106−126. The aromatic-containing ruthenium complexes inhibit peptide aggregation more effectively than other complexes.[34] Platinum complexes in the form of L-$PtCl_2$ inhibit aggregation and toxicity of amyloid-β protein, which provides insights into the therapeutic potential of metal complexes against neurodegenerative disease.[36] Another work studied the interaction between amyloid-β peptide and the complex $[PtCl_2(phen)]$ and found that both platination and noncovalent interaction contribute to the inhibition of Aβ aggregation.[37] Platinum complexes may act as binding agents to neuropeptides for their characteristic coordinating properties. However, little is known about the binding of platinum complexes to PrP106−126.

Since the discovery of the metallopharmaceutical cisplatin, it has remained one of the best-selling anticancer drugs for more than 30 years. Over the past decade, carboplatin and oxaliplatin have been applied in clinical antitumor treatment worldwide.[38−40] Numerous experimental pieces of evidence demonstrate that reactions with proteins are fundamental to determine the overall pharmacological and toxicological profiles of platinum drugs.[41] Cisplatin and carboplatin could bind plasma blood proteins such as albumin and γ-globulin qualitatively and quantitatively.[42−44] During the later stages of reactions of cisplatin with albumin, release of NH_3 occurs due to the strong trans influence of the sulfur atom of methionine, which weakens the Pt−NH_3 bond.[45] Other reports suggest that cisplatin and carboplatin could bind the histidine residue of proteins.[45−48] Recent developments of platinum drugs have extended to nanomaterials for their better transport and loading as metallodrugs.[49]

To explore the effects of platinum complexes on PrP106−126 and its mutant peptides, cisplatin, carboplatin, and $Pt(bpy)Cl_2$ with the same central ion and different ligand configurations were used in the present study (Scheme 1). The results demonstrated that the three platinum complexes bound to the neuropeptides in different binding modes that correlated with the peptide sequence. The binding affinity and inhibitory effect on peptide aggregation of $Pt(bpy)Cl_2$ was stronger than that of cisplatin and carboplatin. Platinum complexes could also rescue the cytotoxicity of SH-SY5Y nerve cells induced by PrP106−126.

Scheme 1. Molecular Structures of $Pt(bpy)Cl_2$, Cisplatin, and Carboplatin

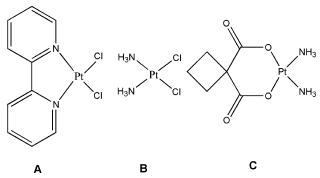

EXPERIMENTAL SECTION

Materials. Human prion protein fragment PrP106−126 and its mutant peptides were chemically synthesized and further purified by SBS Co., Ltd. (Beijing, People's Republic of China). Final products with >95% purity were identified by high-performance liquid chromatography and mass spectrometry (MS). Cisplatin and carboplatin were purchased from Sigma-Aldrich Co., Ltd. The platinum complex $Pt(bpy)Cl_2$ was prepared as described previously and stored at 277 K for further use.[50] All other reagents were of analytical grade.

Electrospray Ionization Mass Spectrometry (ESI-MS). ESI-MS spectra were recorded in the positive mode by directly introducing the samples at a flow rate of 3 μL min^{-1} in an APEX IV FT-ICR high-resolution mass spectrometer (Bruker, USA) equipped with a conventional ESI source. The working conditions were as follows: end plate electrode voltage, −3500 V; capillary entrance voltage, −4000 V; skimmer, 1 and 30 V; dry gas temperature, 473 K. The flow rates of the drying gas and the nebulizer gas were set at 12 and 6 L min^{-1}, respectively. Data analysis 4.0 software (Bruker) was used to acquire data. Deconvoluted masses were obtained using an integrated deconvolution tool. The peptide sample used in ESI-MS experiments was kept constant at 50 μM. Different molar ratios of $Pt(bpy)Cl_2$, cisplatin, and carboplatin were added to the sample for valid assays.

NMR Spectroscopy. ^1H NMR experiments were performed on a Bruker Avance 400 MHz spectrometer at 298 K. The samples were prepared by adding a stock solution of the metal compound to the peptide solution at different molar ratios, which contained 10% d_6-DMSO in H_2O. The final peptide concentration was 0.5 mM. The pH value was carefully adjusted to 5.7 with either DCl or NaOD. A watergate pulse program with gradients was applied to suppress the residual water signal. All NMR data were processed by Bruker Topspin 2.1 software.

Spectrofluorometric Measurements. Steady-state fluorescence measurements of the intrinsic phenylalanine residue were carried out at room temperature to further compare the binding ability of platinum complex to prion peptides. The excitation wavelength of 260 nm was chosen according to a previous report.[51] The dissociation constant (K_d) was determined from the plot of fluorescence intensity via the platinum complex concentration using the following equation

$$\Delta F = F_0 - F_L = (F_0 - F_a)\{K_d + P_0 + T - [(K_d + P_0 + T)^2 - 4P_0T]^{1/2}\}/2P_0 \quad (1)$$

dx.doi.org/10.1021/ic500092t | Inorg. Chem. 2014, 53, 5044−5054

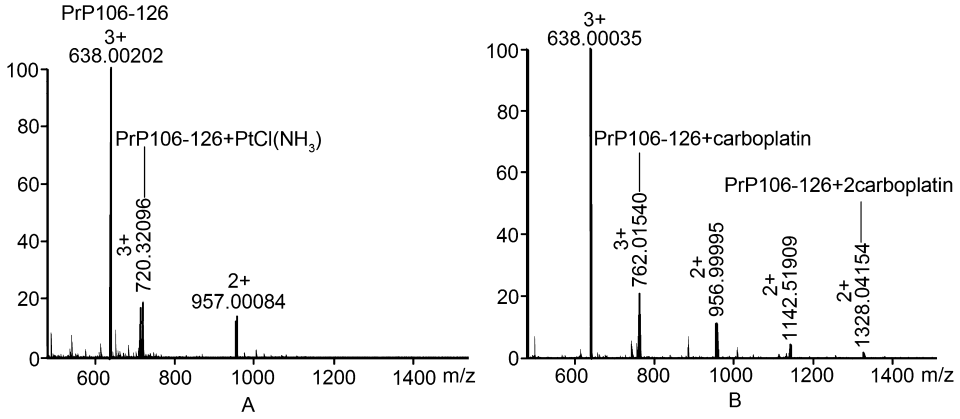

Figure 1. ESI-MS spectra of PrP106−126 in the presence of cisplatin (A) and carboplatin (B). The aqueous solution was prepared by adding double amounts (molar ratio) of cisplatin and quintuple amounts of carboplatin to the peptide. The final concentration of the peptide was 50 μM.

where F_0 and F_L are the measured fluorescence intensities of peptides at 287 nm in the absence and presence of platinum complex.[52,53] F_α is the maximum quenching of the peptide fluorescence. P_0 stands for the initial concentration of peptide, and T represents the concentration of added platinum complex. Three Phe-containing peptides were used in this study, and the concentration for each was 100 μM. The results were obtained from three repeated experiments.

Thioflavin T (ThT) Assay. The peptides were aged for 24 h, and then the complex Pt(bpy)Cl_2 in the concentration range of 25−200 μM was incubated with the peptide and its mutant peptides in a 10 mM phosphate buffer at pH 7.2. After 24 h incubation of the mixture, the sample was added with 0.1 mM ThT, and its fluorescence was monitored using an F-4600 spectrofluorometer (Hitachi Ltd., Japan). The ThT fluorescence signal was quantified by determining the average of fluorescence emissions at 500 nm for 10 s at an excitation of 432 nm. For cisplatin and carboplatin, the concentration ranges were expanded to 300 and 500 μM, respectively. The reported data were the average of three experiments.

Atomic Force Microscopy (AFM). Samples were prepared by mixing 1 mM peptide solution with different ratios of platinum complexes and then incubated at 310 K for 24 h. The final peptide concentration used in the AFM experiment was 0.1 mM with 1% dimethyl sulfoxide. Images were obtained in tapping mode with a silicon tip under ambient conditions, a scanning rate of 1 Hz, and a scanning line of 512 using a Veeco D3100 instrument (Veeco Instruments 151, Inc., USA).

MTT Assay. Human SH-SY5Y neuroblastoma cells were cultured in a 1:1 mixture of Dulbecco's modified Eagle's medium and F12 medium supplemented with 10% fetal bovine serum, 2 mM glutamine, 100 U mL^{-1} penicillin, and 100 U mL^{-1} streptomycin. Cells were maintained at 310 K in a humidified incubator under 95% air and 5% CO_2. Cell survival was assessed by measuring the reduction of 3-(4,5-dimethylthiazol-2-yl)-2,5-diphenyltetrazolium bromide (MTT). Up to 100 μM PrP106−126 was incubated for 24 h with or without 100 μM platinum complexes, and then the mixtures were added to the cells. After 4 days of reaction, the cells were incubated with 10 μL MTT at 310 K for 4 h. The absorbance at 570 nm was recorded with a Cary 50 UV−vis spectrophotometer (Varian, Inc., USA). Each experiment was carried out in quadruplicate. The data were calculated as percentages of untreated control value.

RESULTS

ESI-MS Spectra of Prion Peptides with Platinum Complexes. To determine if the platinum complexes would bind directly to prion peptides and to identify the probable binding pattern between these substances, different amounts of Pt(bpy)Cl_2, cisplatin, and carboplatin were incubated with the peptides. The final solution was analyzed by ESI-MS. The addition of Pt(bpy)Cl_2 caused the formation of the adduct [PrP106−126+Pt(bpy)], in accordance with that reported previously (Figure S1, Supporting Information).[32] The free PrP106−126 exhibited an intense peak of 638.00 (3+) corresponding to its expected mass. Double amounts of cisplatin were incubated with the peptide and formed [PrP106−126+PtCl(NH_3)], as indicated by the peak of 720.32 (2+) (Figure 1A). The adduct of the prion peptide and the fragment PtCl(NH_3) indicated that the cisplatin may coordinate the peptide with one chlorine atom and one amidogen split off. After incubating quintuple amounts of carboplatin with PrP106−126, two peaks referring to the adduct of [PrP106−126+carboplatin] [762.02 (3+)] and [PrP106−126 + 2carboplatin] [1328.04 (2+)] were detected (Figure 1B).

For the mutant peptides H111A, M112 V, and M109F/H111A, the complex Pt(bpy)Cl_2 bound to the peptides in the form [peptide+Pt(bpy)] (Figure 2). In contrast, for the mutants M109F/M112 V and M109F, the new adduct formed by the addition of Pt(bpy)Cl_2 was detected as [peptide+Pt(bpy)Cl_2] (Figure 2). Otherwise, the complex bound to the peptide H111A/M112 V in the form of Pt(bpy)Cl, forming the adduct [H111A/M112 V+Pt(bpy)Cl].

The incubation of equivalents of cisplatin or carboplatin with mutant peptides showed no binding adducts because the binding affinity between these two complexes and peptides was weak. After double amounts of cisplatin were added to H111A, cisplatin bound to the peptide in the form of Pt(NH_3)$_2$ and PtCl(NH_3), corresponding to the adducts [H111A+Pt(NH_3)$_2$] and [H111A +PtCl(NH_3)]. For the peptide M109F/M112 V, cisplatin bound to the peptide in intact form, as [M109F/M112 V+PtCl$_2$(NH_3)$_2$]. For all the other mutant peptides, cisplatin bound to the peptides in the same intact form. A distinctive phenomenon was that the 2:1 binding adduct was detected between the compound and four short peptides (Figure 3). Quintuple amounts of carboplatin were also incubated with the six mutant peptides. The final adducts were represented in 1:1, 2:1, and 3:1 ratio binding modes (Figure S2, Supporting Information). Table 2 shows a detailed illustration of the MS data after incubating the three complexes with the prion peptides. ESI-MS showed that platinum complexes may bind to the peptides in different binding modes.

^{1}H NMR Studies on the Interactions of Platinum Complexes with Prion Peptides. The ^{1}H NMR spectrum of PrP106−126 was acquired, and the characteristic peaks from side chains of His111 and Met109/112 were identified as reported.[28,34] Pt(bpy)Cl_2 and cisplatin caused the broadening of His111 C_δHs at 7.08 ppm, and the signal intensity at 2.08 ppm assigned to Met109/112 C_ϵHs was clearly decreased, indicating

dx.doi.org/10.1021/ic500092t | Inorg. Chem. 2014, 53, 5044−5054

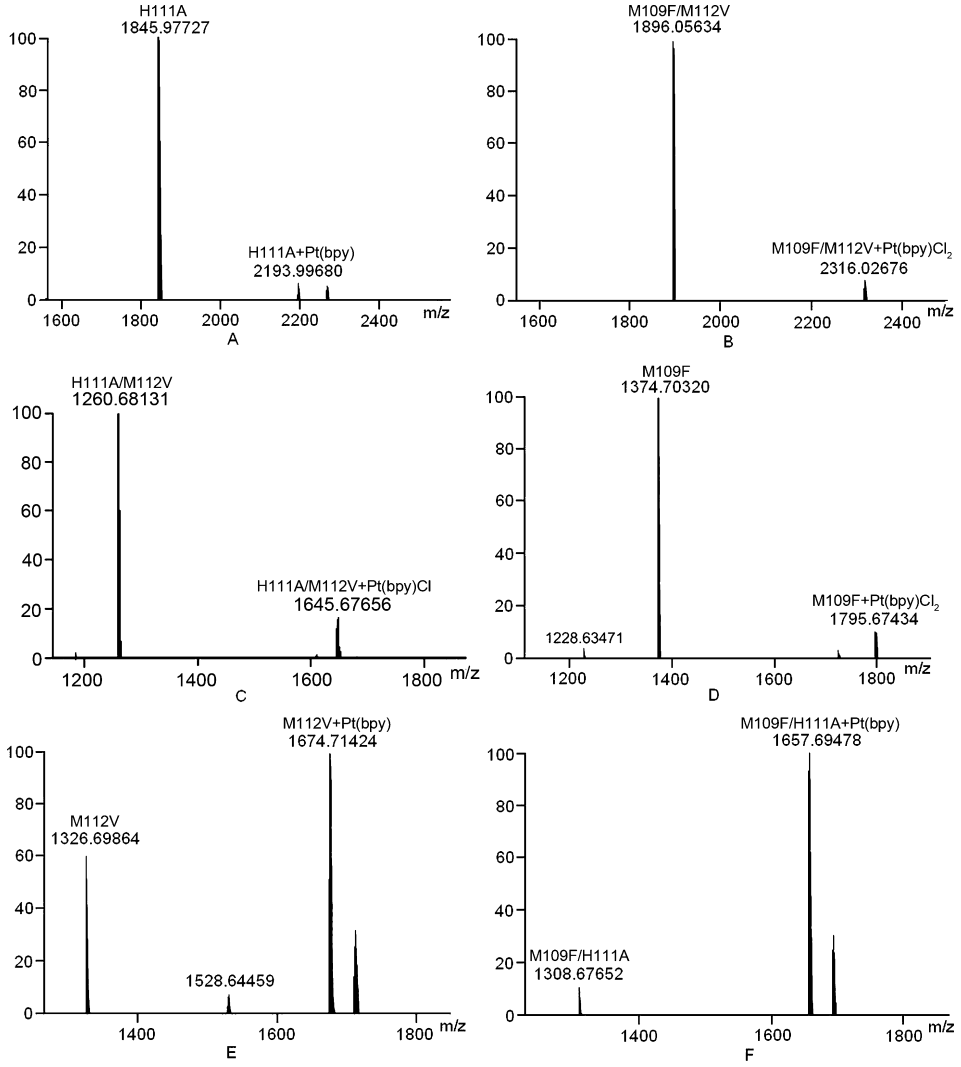

Figure 2. ESI-MS spectra of PrP106−126 mutants in the presence of an equivmolar amount of $Pt(bpy)Cl_2$ (from left to right and top to bottom): (A) H111A; (B) M109F/M112 V; (C) H111A/M112 V; (D) M109F; (E) M112 V; (F) M109F/H111A. The final concentration of the peptide was 50 μM.

that the binding sites for $Pt(bpy)Cl_2$ and cisplatin may include His111 and Met109/112 (Figure 4). In contrast, the signals of His111 C_δHs or Met C_ϵHs were less affected on treatment of carboplatin. Although carboplatin has a reaction mode similar to that of cisplatin according to the ESI-MS data, the different results in NMR spectra may be attributed to the slow reaction of carboplatin with the peptides.

The histidine-mutated prion peptide H111A showed a distinct NMR spectrum in comparison with that of PrP106−126. With the addition of $Pt(bpy)Cl_2$ and cisplatin, the upfield resonance peak at 2.08 ppm decreased, indicating the binding of Met109 or Met112 with platinum complexes (Figure S3, Supporting Information). Carboplatin had less effect on the ^{1}H NMR spectrum of peptide H111A; no featured peak was observed. For the peptide M109F/M112 V, the addition of $Pt(bpy)Cl_2$ and cisplatin caused the variation of signals from His111 and Phe109 (at 7.20 and 7.30 ppm, respectively). In comparison, the complex carboplatin did not exert a disturbance on the signal of His111 C_δHs (Figure S4, Supporting Information).

For the four short peptides, incubation of platinum complexes with the peptide M109F led to differing spectra, in which the signal of His111 C_δHs was not effectively affected by $Pt(bpy)Cl_2$ except for a slight decrease. Cisplatin caused the broadening and decrease of His111 C_δHs and Met112 C_ϵHs (Figure S5, Supporting Information). On the other hand, the signal of Met109 in H111A/M112 V was not as notably influenced after incubating the complexes with the peptide (Figure S6, Supporting Information). Moreover, the addition of platinum complexes caused negligible disturbance on the signals of M112 V (Figure S7, Supporting Information). The spectrum of peptide M109F/H111A changed little with the treatment of platinum complexes (Figure S8, Supporting Information).

Fluorescence Measurements of Phe-Containing Peptides Binding to Platinum Complexes. The method of fluorescence quenching has been utilized to calculate K_d in numerous studies.[31,54,55] The change in peptide fluorescence upon adding a platinum complex can be assumed to reflect the amount of complex produced. The fluorescence quenching of phenylalanine residue can represent structural changes brought about by a platinum complex. The fluorescence intensity of the peptide at 287 nm in the presence of a platinum complex was therefore used to estimate K_d by means of a nonlinear-least-squares regression using eq 1 (Figure 5).

The three Phe-containing mutant peptides M109F/M112 V, M109F, and M109F/H111A were used to compare their binding affinity to platinum complex. No K_d data were supplied for other

dx.doi.org/10.1021/ic500092t | Inorg. Chem. 2014, 53, 5044−5054

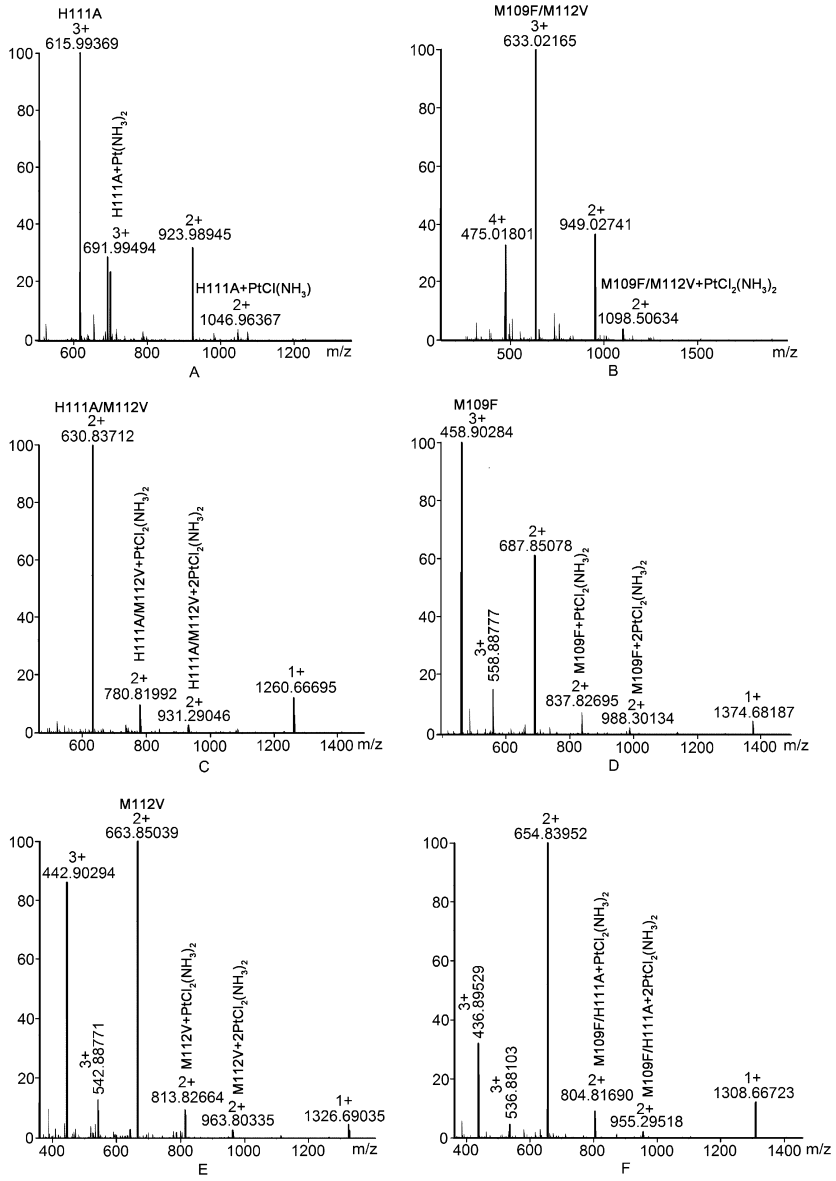

Figure 3. ESI-MS spectra of PrP106−126 mutants in the presence of double amounts (molar ratio) of cisplatin; (from left to right and top to bottom): (A) H111A; (B) M109F/M112 V; (C) H111A/M112 V; (D) M109F; (E) M112 V; (F) M109F/H111A. The final concentration of the peptide was 50 μM.

peptides used in this work because of their lack of fluorescent residue. In order to observe the binding kinetics, the experiments were carried out by mixing three platinum complexes with M109F/M112 V, respectively. The results showed that the fluorescence intensity for $Pt(bpy)Cl_2$ stabilized within a very short equilibrium time, whereas the variation of fluorescence intensity for cisplatin and carboplatin was prolonged to almost 2 h (Figure S9, Supporting Information). The observed K_d value was $(6.2 \pm 1.4) \times 10^{-6}$ M for $Pt(bpy)Cl_2$ to the peptide M109F/M112 V, and K_d was $(6.4 \pm 1.1) \times 10^{-6}$ and $(9.6 \pm 1.2) \times 10^{-6}$ M for $Pt(bpy)Cl_2$ to M109F and M109F/H111A, respectively. However, the K_d values of cisplatin and carboplatin with the peptides were not provided because of their slow reaction.

Aggregation Inhibition Induced by Platinum Complex−ThT Assay of Prion Peptides. PrP106−126 is essential to PrP^{Sc} aggregation, which is correlated with the neurotoxicity of prion proteins. The aggregation of PrP106−126 can be monitored by a ThT assay, as noted in earlier reports.[56,57] In order to assess the influence of platinum complexes on the ThT fluorescence, a control experiment was performed. The result showed that platinum complexes had little impact on the ThT fluorescence (Figure S10, Supporting Information). Figure 6 and Figure S11 (Supporting Information) show the change in fluorescence signal when serial platinum complexes were added to the peptides. The ThT fluorescence intensity decreased after platinum complexes were incubated with prion peptides, suggesting that fibril formation was inhibited. PrP106−126 aggregation was more effectively inhibited by $Pt(bpy)Cl_2$, with an IC_{50} value of 32 ± 4 μM. By comparison, cisplatin and carboplatin inhibited the peptide relatively more weakly than $Pt(bpy)Cl_2$, with IC_{50} values at 52 ± 5 and 113 ± 10 μM, respectively. The platinum complexes exhibited similar fluorescence quenching to the mutant peptides H111A and M109F/M112 V, where the ThT fluorescence intensity also decreased after the peptide was incubated with platinum complexes. Table 3 shows a concrete description of the IC_{50} value for the inhibitory effect of platinum complexes on amyloidogenic prion

dx.doi.org/10.1021/ic500092t | Inorg. Chem. 2014, 53, 5044−5054

Table 2. ESI-MS Values of Peptides with the Platinum Complexes and the Corresponding Bound Species Calculated

	PrP106−126	H111A	M109F/M112 V	H111A/M112 V	M109F	M112 V	M109F/H111A
$Pt(bpy)Cl_2$							
calcd	2260.24 (1+)	2194.22 (1+)	2317.21 (1+)	1646.38 (1+)	1795.85 (1+)	1676.95 (1+)	1658.93 (1+)
measd	2260.02 (1+)	2194.00 (1+)	2316.03 (1+)	1645.68 (1+)	1795.67 (1+)	1674.71 (1+)	1657.69 (1+)
cisplatin							
calcd	2158.54 (1+)	2074.10 (1+), 2092.52 (1+)	2195.08 (1+)	1559.71 (1+), 1859.76 (1+)	1673.03 (1+), 1973.78 (1+)	1625.73 (1+), 1925.78 (1+)	1607.71 (1+), 1907.76 (1+)
measd	720.32 (3+)	692.00 (3+), 1046.96 (2+)	1098.51 (2+)	780.82 (2+), 931.29 (2+)	837.83 (2+), 988.30 (2+)	813.83 (2+), 963.80 (2+)	804.82 (2+), 955.30 (2+)
carboplatin							
calcd	2282.23 (1+), 2653.48 (1+)	2216.21 (1+), 2587.46 (1+), 2958.70 (1+)	2266.29 (1+), 2637.54 (1+), 3008.78 (1+)	1630.92 (1+), 2002.17 (1+), 2373.42 (1+)	1744.94 (1+), 2116.19 (1+), 2487.44 (1+)	1696.94 (1+), 2068.19 (1+), 2439.44 (1+)	1678.92 (1+), 2050.17 (1+), 2421.42 (1+)
measd	762.02 (3+), 1328.04 (2+)	1109.51 (2+), 1295.03 (2+), 1480.55 (2+)	1134.54 (2+), 1320.06 (2+), 1505.58 (2+)	816.86 (2+), 1002.38 (2+), 1187.90 (2+)	873.87 (2+), 1059.40 (2+), 1244.92 (2+)	849.87 (2+), 1034.89 (2+), 1220.92 (2+)	840.86 (2+), 1026.38 (2+), 1121.90 (2+)

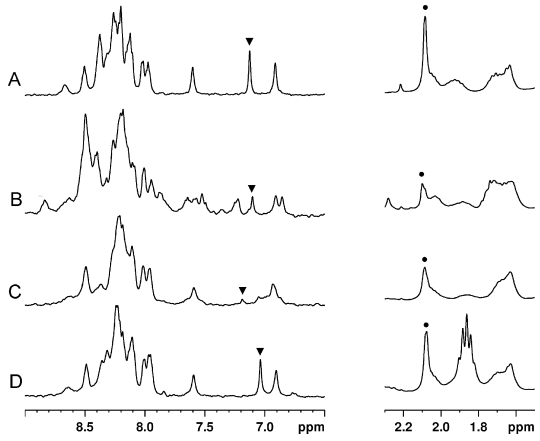

Figure 4. ^1H NMR spectra of 0.5 mM PrP106−126 in H_2O/d_6-DMSO at pH of 5.7 and 298 K: (A) PrP106−126 alone; (B−D) PrP106−126 in the presence of an equimolar amount of $Pt(bpy)Cl_2$ (B), 2.0 equiv of cisplatin (C), and 5.0 equiv of carboplatin (D). The peak marked with a solid circle at 2.08 ppm is from a C_εHs group of methionine and the peak marked by an inverted triangle at 7.08 ppm is from the C_δHs of His111. The peak of 1.86 ppm in D is from carboplatin.

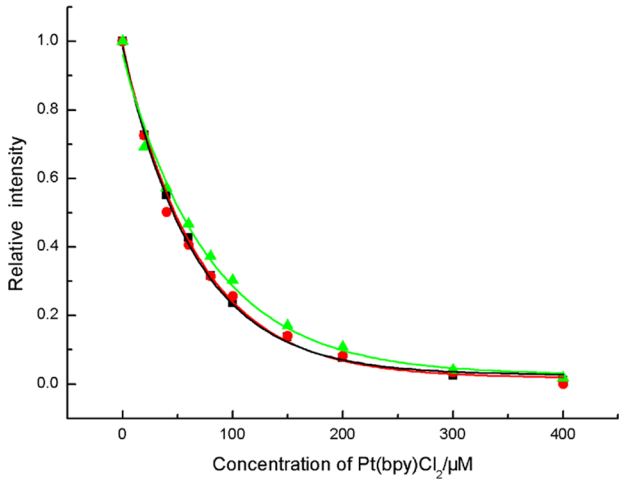

Figure 5. Intrinsic fluorescence spectra of M109F/M112 V (black), M109F (red), and M109F/H111A (green) plotted at 287 nm on titration with $Pt(bpy)Cl_2$. The concentration of the peptide was 100 μM.

peptides. The short 14aa peptides could not self-aggregate; thus, no data are provided for them.

AFM Images of Prion Peptide Aggregation. AFM was performed to verify if the platinum complexes affect peptide aggregation and fibril formation. The average result of the three experiments was described. The aggregates formed by PrP106−126 had a dense fibrillar structure (Figure 7A), which suggested a strong aggregation state after 24 h of incubation at 310 K. However, AFM micrographs of PrP106−126 in the presence of platinum complexes showed that such aggregation was reversed. $Pt(bpy)Cl_2$ influenced PrP106−126 aggregation more effectively than cisplatin and carboplatin (Figure 7B−D). The fibrils formed by H111A differed in terms of shape and morphology from those of PrP106−126, and the inhibitory effect of $Pt(bpy)Cl_2$ was stronger than those of the other complexes (Figure 8). The aggregates formed by M109F/M112 V showed aggregation stronger than that of H111A but weaker than that of PrP106−126. $Pt(bpy)Cl_2$ changed the aggregates to short hairlike filaments, whereas cisplatin and carboplatin did not reverse the

dx.doi.org/10.1021/ic500092t | Inorg. Chem. 2014, 53, 5044−5054

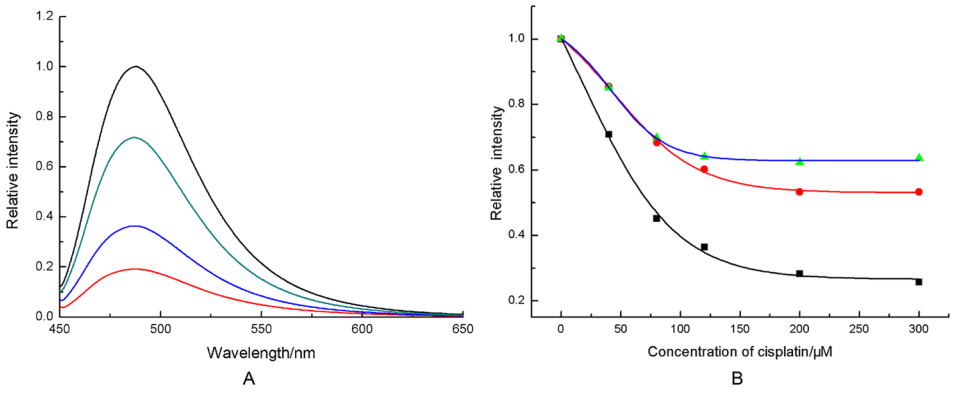

Figure 6. (A) Evaluation of the ability of $Pt(bpy)Cl_2$ (red), cisplatin (blue), and carboplatin (green) to inhibit the aggregation of PrP106−126. The concentration of the platinum complexes was 100 mM. (B) Ability of cisplatin to inhibit the aggregation of PrP106−126 (black), H111A (green), and M109F/M112 V (red) measured by a thioflavin T (ThT) fluorescence assay.

Table 3. IC_{50} Values for the Inhibition of Aggregation of Platinum Complexes on PrP106−126 and Its Mutants Measured with ThT Fluorescence

	$Pt(bpy)Cl_2$	cisplatin	carboplatin
PrP106−126	32 ± 8	52 ± 5	113 ± 10
H111A	29 ± 3	56 ± 6	72 ± 7
M109F/M112 V	27 ± 3	56 ± 9	102 ± 14

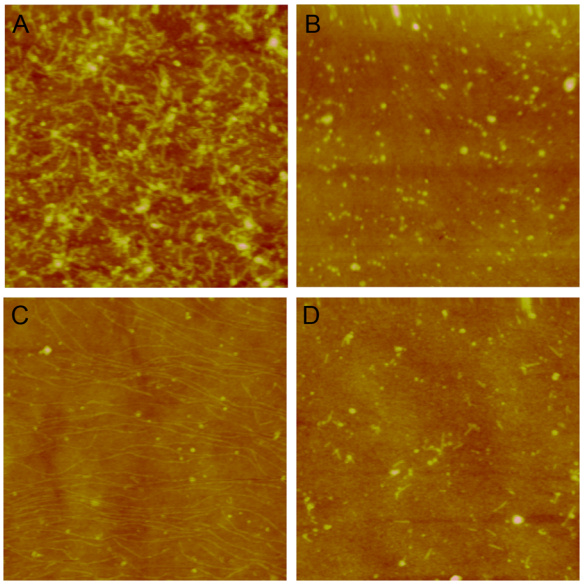

Figure 7. Atomic force microscopy images of PrP106−126 in the absence (A) and in the presence of an equimolar amount of $Pt(bpy)Cl_2$ (B), a double amount of cisplatin (C), and a quintuple amount of carboplatin (D). The peptide concentration for the final assay was 10 μM.

aggregation effectively (Figure S12, Supporting Information). The results of AFM images agreed with those of the ThT assay.

Neurotoxicity of PrP106−126 Regulated by Platinum Complexes. Platinum complexes can bind with prion neuropeptide PrP106−126 and its mutants and modify their aggregation behavior significantly. The ability of platinum complexes to reduce the neurotoxicity of PrP106−126 was assessed using human SH-SY5Y neuroblastoma cells. Cell survival was evaluated after treating the SH-SY5Y cells with the peptide alone or with the peptide and platinum complex together. In comparison with the control sample, PrP106−126

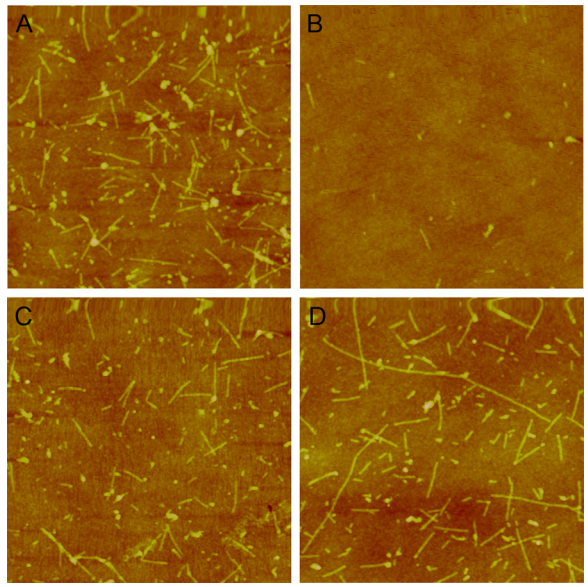

Figure 8. Atomic force microscopy images of peptide H111A in the absence (A) and presence of an equimolar amount of $Pt(bpy)Cl_2$ (B), a double amount of cisplatin (C), and a quintuple amount of carboplatin (D). The peptide concentration for the final assay was 10 μM.

caused a remarkable decrease of cell viability to 36%, as measured by an MTT assay. The addition of $Pt(bpy)Cl_2$ to PrP106−126 increased the cell viability to 66% (Figure 9), whereas for cisplatin and carboplatin, the cell viability of SH-SY5Y reverted to 68% and 54%, respectively. Notably, the self-toxicity of the three platinum complexes to SH-SY5Y cells was not high (Figure S13, Supporting Information), but they may restore the neurotoxicity induced by PrP106−126 effectively.

DISCUSSION

PrP106−126 is an acceptable model for research of PrP^{Sc} because of their similar physicochemical and biological properties. A number of potential reagents have been studied to inhibit the aggregation and neurotoxicity of PrP106−126 in various ways, which include small organic molecules, inorganic metal complexes, and mimical chaperones. However, great efforts must be exerted to unravel the interaction mechanism of inhibitors with prion peptides to design and develop potential drugs against prion disease. The present work focuses on platinum complexes with different ligand configurations that

dx.doi.org/10.1021/ic500092t | Inorg. Chem. 2014, 53, 5044−5054

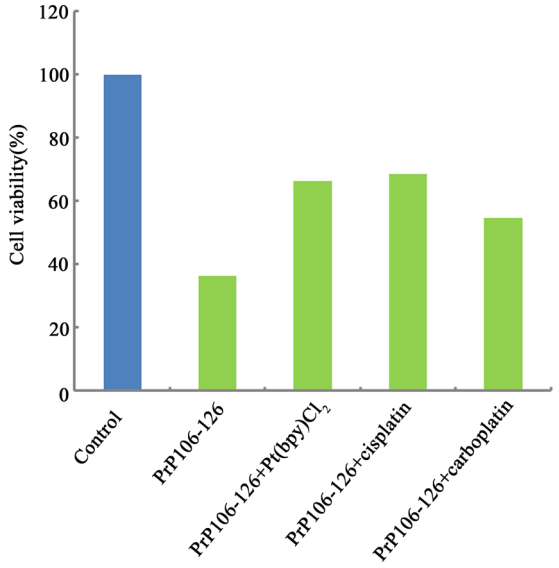

Figure 9. Effect of platinum complexes on the neurotoxicity of PrP106−126. Cell viability was determined by an MTT assay. The data represent the average of four experiments. Incubation of platinum complexes with PrP106−126 inhibited the cellular toxicity of the peptide.

inhibit the amyloidogenic properties of PrP106−126 and its mutants. The interaction between platinum complexes and the prion peptides relied on the peptide sequence, the molecular structure of metal complexes, and the methionine residue, which was a preferential site for the platinum complexes.

Characteristic Binding Modes of Platinum Complexes with Prion Peptides. Cisplatin and carboplatin are well-known metallo-pharmaceutical drugs for cancer treatment.[38,40,58] The mechanism of the two reagents appears to bind to cellular DNA, resulting in selective inhibition of new DNA synthesis.[58] However, they may also bind with proteins such as albumin and γ-globulin, which induce harmful side effects.[41−44] Cisplatin binds human serum albumin through the polypeptide C−N, C═O, and sulfur donor groups, which ultimately changes the secondary structure of HSA.[43] Cisplatin and carboplatin were used in this study to determine if a different ligand configuration could affect the biophysical properties of PrP106−126 and its mutants, in comparison with aromatic $Pt(bpy)Cl_2$. The binding modes of different platinum complexes with prion peptides were determined through MS and NMR spectroscopy.

Evaluation of ESI-MS data illustrated that platinum complexes may coordinate with the peptide only if the methionine residue is situated in the peptide sequence. Earlier reports showed that $Pt(bpy)Cl_2$ platinates with PrP106−126 in the form of "Pt(bpy)", referring to the split of two chlorines and the retainment of the bipyridine ligand.[32] The ^{1}H NMR result showed that $Pt(bpy)Cl_2$ may be bound to side-chain nitrogen and sulfur atoms of His111 and Met109/112, as remarkable changes in the characteristic peaks were observed. In the case of cisplatin, it bound to PrP106−126 as $[PrP106−126+PtCl(NH_3)]$, indicating the coordination of the central ion with the peptide, which was also verified by an NMR assay. In contrast, carboplatin bound to the peptide with an intact molecule, indicating a binding mode different from that of $Pt(bpy)Cl_2$ and cisplatin. The negligible change of His111 C_δHs and Met C_εHs also implied a different binding mode in comparison with the other two complexes.

Different kinds of nonbonded interactions were assumed. To further elucidate the binding reactions of platinum complexes with prion peptides, six other peptides in which the residues Met109, His111, and Met112 selectively mutated were chosen for the purpose. From the ESI-MS spectra, we may deduce that H111A bound $Pt(bpy)Cl_2$ in the same way as PrP106−126. In contrarst, the mutants M109F/M112 V and M109F both bound the complex in the form of $[peptide+Pt(bpy)Cl_2]$, whereas M112 V and M109F/H111A bound $Pt(bpy)Cl_2$ in the same way as for native PrP106−126 and H111A. Moreover, the changes of His111 C_δHs and Phe109 C_δHs observed in the NMR spectrum of peptide M109F/M112 V might be attributed to coordination of $Pt(bpy)Cl_2$ with the residues, though the bound species were not detected in MS. Similarly, when cisplatin bound to M112 V and M109F/H111A in a nonbonded mode, the unconspicuous change of Met peak was also observed, as shown in Figures S7 and S8 (Supporting Information).

The diversity may have been contributed by the common difference of the peptide sequence and the specific coordinating tendency of platinum. For the complexes $Pt(bpy)Cl_2$ and cisplatin, the noncovalent binding may depend on the peptide sequence, because coordination is more preferable if Met109 or/and Met112 exist in the peptide sequence. NMR data also showed that the absence of Met112 would make cisplatin less inclined to coordinate with the peptide (Figure S7, Supporting Information). In contrast, the complex carboplatin bound all the peptides in an intact form. This may result from its unique ligand configuration and a very slow dissociation of the complex in solution. It is likely that carboplatin interacted with peptides before it underwent hydrolysis. Comparing the current applied peptide sequence with MS and NMR data, we could make a preliminary speculation that platinum complexes are inclined to coordinate the methionine residue, especially Met112. Another speculation is that the presence of His111 may help $Pt(bpy)Cl_2$ coordinate with peptides, although His111 is more important for the binding of gold complexes to PrP106−126.[33]

The incubation of cisplatin with the six mutant peptides further supported the speculation above. Cisplatin coordinated with the peptides PrP106−126 and H111A, whereas it bound to other peptides in the same way as carboplatin did in an intact combined molecule. This finding suggested that cisplatin coordinated with the peptide mainly by residue Met109 and/or Met112, but not His111 in advance. Although cisplatin platinated HSA in the positions of Cys, Met, Tyr, and Asp residues,[41] and other studies have demonstrated that both cisplatin and carboplatin could bind C_δH and C_εH of His15 in hen egg-white lysozyme (HEWL),[45−48] the present work elucidated that the His residue showed a weaker coordinating ability in comparison with Met residue among the currently applied prion peptides.

Different Binding Affinities of Platinum Complexes with Prion Peptides. $Pt(bpy)Cl_2$ bound to PrP106−126 and H111A through a coordinated interaction with release of free chlorines. The central platinum ion possibly coordinated with the sulfur of Met109/112 and side-chain nitrogen of His111, as indicated by NMR data. For effective detection of cisplatin reacting with H111A in double amounts in MS experiments, the new bound species $[H111A+PtCl(NH_3)]$ may have also been caused by its covalent binding with the peptide but had weaker binding affinity than $Pt(bpy)Cl_2$. However, cisplatin bound to the other peptides in a new manner, wherein no atom was released from the complex. This finding elucidated that noncovalent binding existed during the binding process. A quintuple amount of carboplatin also bound to all the peptide species in the form of intact molecules. Amine ligands in

dx.doi.org/10.1021/ic500092t | Inorg. Chem. 2014, 53, 5044−5054

carboplatin are considered "non-leaving" ligands or inactive ligands owing to the established sequence of metal−ligand bond strength.[40] Thus, the binding affinity between carboplatin and the peptide was further weakened.

The binding affinity between the platinum complexes and the peptides was further estimated by an intrinsic phenylalanine fluorescence quenching assay. In comparison with MS and NMR data, we know that the binding of $Pt(bpy)Cl_2$ to those peptides was contributed by both metal coordination and a nonbonded interaction. The binding kinetics of cisplatin/carboplatin with the peptide showed a slow reaction, and the binding was contributed mainly by a nonbonded interaction, as reflected by MS analysis. Perhaps the binding mode was affected by the dissociation rate of the ligand in solution as well as the peptide sequence.

Effective Inhibition of Platinum Complexes on Aggregation of Prion Peptides. A possible pathogenesis of prion disease is the infection of PrP^{Sc} with cellular PrP^{C}. Thus, resistance of PrP^{Sc} formation and inhibition of its aggregation are crucial. The C-terminal hydrophobic residues are mainly responsible for the peptide aggregation. Comparing the aggregation behavior of WT PrP106−126, H111A, and M109F/M112 V (Figures 7, 8 and Figure S12 (Supporting Information)), we may find that the mutant H111A could still aggregate into fibrils with the existence of Met109 and Met112, but with a weaker extent of aggregation ability than WT PrP106−126. This means that His111 has a vital impact on the peptide aggregation. For the mutant M109F/M112 V, the aggregation ability was not obviously weakened in comparison with the WT peptide. This indicates that existence of Met residues correlate with the peptide aggregation to some extent.

A bold assumption was made: namely, the interaction between platinum complexes and pathological proteins could control the behavior of the proteins. An AFM assay shed light on the effective role of platinum complexes in inhibiting the aggregation of prion peptides. The complex $Pt(bpy)Cl_2$ could reverse the aggregated PrP106−126 into scattered oligomers under equivalent mixing. By comparison, cisplatin affected the peptide fibril at a lower level even at a double amount, as long hairlike fibrils could still be observed. When a quintuple amount of carboplatin was incubated with the peptide, the inhibitory effect was relatively stronger than that of cisplatin when protofibrils were detected.

The mutant 21aa peptide H111A could self-aggregate, and an aggregation state weaker than that of PrP106−126 was shown. $Pt(bpy)Cl_2$ reversed the aggregation of H111A to the greatest extent, with only a few oligomers observed. However, the inhibitory effect of cisplatin and carboplatin on the aggregation of H111A decreased more noticeably than that of $Pt(bpy)Cl_2$. The binding affinity and inhibitory effect of the complexes did not seem to coordinate with that of peptide H111A. This conflict may have been driven by the small ligand of cisplatin, which had less contribution to the aggregation properties of H111A than $Pt(bpy)Cl_2$. When cisplatin was applied to another 21aa peptide, M109F/M112 V, the self-aggregation degree was weaker than that of PrP106−126 but stronger than that of H111A. The inhibition of $Pt(bpy)Cl_2$ and cisplatin on the aggregation of M109F/M112 V was not obvious because of its small oligomer state, but tiny scattered fibrils of the peptide were observed. Another similarity between H111A and M109F/M112 V was the weaker inhibitory effect of carboplatin in comparison with the two other complexes.

With regard to the peptide sequence, the results indicated that His111 and Met109/112 are important residues for PrP106−126. The lack of C-terminals also led to the inability of prion peptide aggregation. Aromatic $Pt(bpy)Cl_2$ showed better inhibition on the aggregation of prion peptides through mainly metal coordination. The ligand configuration influenced the inhibitory effects by the ligands' "inactive" behavior, as seen in carboplatin. On the other hand, it should be noted that both coordination and nonbonded interactions contribute to the inhibition of peptide aggregation. Cisplatin and carboplatin primarily bind to the peptides by nonbonded interactions, and their inhibitory effects on peptide aggregation are weaker than that of $Pt(bpy)Cl_2$.

Regulation of Platinum Complexes on Neurotoxicity of PrP106−126. PrP106−126 drastically reduces the cell viability in primary cultures of hippocampal, cortical, and cerebellar neurons.[11,59] Treatment of PrP106−126 with human SH-SY5Y cells induces a concentration- and time-dependent decrease of the number of active neuroblastoma cells.[60−62] In the present study, the cell death induced by PrP106−126 (100 μM) after 4 days of treatment with the hSH-SY5Y cells was 37%, similar to previous reports.[60−62] Under the same incubation conditions, the addition of $Pt(bpy)Cl_2$ rescued the neurotoxicity of PrP106−126 by up to 30%, and the final cell viability was 66%. Cisplatin reversed the toxicity of the peptide to 68%, better than that of carboplatin (54%), which may be attributed to a different binding affinity with the peptide. Although the regulatory ability of $Pt(bpy)Cl_2$ on the neurotoxicity of PrP106−126 was comparable with that of cisplatin, it is still one of the potential inhibitors, given its great binding affinity and better inhibitory effect on peptide aggregation.

In summary, the present study showed that platinum complexes could bind to prion peptides through coordination and nonbonded interactions. A comparison of the binding affinity among different peptides indicated that methionine residue, rather than histidine residue, was preferred over the platinum complexes, representing a sulfophile characteristic of platinum. The inhibitory effects of platinum complexes on the aggregation and neurotoxicity behavior of prion peptides were also identified. The results revealed that a different ligand configuration is crucial for both the binding affinity and the inhibition of peptide fibril formation, and metal complexes are particularly promising as potential drugs against prion disease.

■ ASSOCIATED CONTENT

Supporting Information

Figures giving ESI-MS data, fluorescence spectra, and atomic force microscopy of peptide interactions with platinum complexes. This material is available free of charge via the Internet at http://pubs.acs.org.

■ AUTHOR INFORMATION

Corresponding Author

*E-mail for W.D.: whdu@chem.ruc.edu.cn.

Author Contributions

The manuscript was written through contributions of all authors. All authors have given approval to the final version of the manuscript.

Notes

The authors declare no competing financial interest.

■ ACKNOWLEDGMENTS

This work was supported by the National Natural Science Foundation of China (No. 21271185), the National Basic

Research Program (No. 2011CB808503), the Fundamental Research Funds for the Central Universities, and the Research Funds of Renmin University of China (No.14XNH059).

REFERENCES

(1) Prusiner, S. B. *Science* **1997**, *278*, 245−251.
(2) Prusiner, S. B. *Proc. Natl. Acad. Sci. U.S.A.* **1998**, *95*, 13363−13383.
(3) Zhou, Z.; Xiao, G. *Acta Biochim. Biophys. Sin.* **2013**, *45*, 465−476.
(4) Jackson, G. S.; Hosszu, L. L. P.; Power, A.; Hill, A. F.; Kenney, J.; Saibil, H.; Craven, C. J.; Waltho, J. P.; Clarke, A. R.; Collinge, J. *Science* **1999**, *283*, 1935−1937.
(5) Brown, K.; Mastrianni, J. A. *J. Geriatr. Psychiatry Neurol.* **2010**, *23*, 277−298.
(6) Bocharova, O. V.; Breydo, L.; Parfenov, A. S.; Salnikov, V. V.; Baskakov, I. V. *J. Mol. Biol.* **2005**, *346*, 645−659.
(7) Hu, P. P.; Huang, C. Z. *Acta Biochim. Biophys. Sin.* **2013**, *45*, 435−441.
(8) Walsh, P.; Simonetti, K.; Sharpe, S. *Structure* **2009**, *17*, 417−426.
(9) Salmona, M.; Malesani, P.; Gioia, L. D.; Gorla, S.; Bruschi, M.; Molinari, A.; Vedova, F. D.; Pedrotti, B.; Marrari, M. A.; Awan, T.; Bugiani, O.; Forloni, G.; Tagliavini, F. *Biochem. J.* **1999**, *342*, 207−214.
(10) Vilches, S.; Vergara, C.; Nicolás, O.; Sanclimens, G.; Merino, S.; Varón, S.; Acosta, G. A.; Albericio, F.; Royo, M.; Del Río, J. A.; Gavín, R. *PLoS One* **2013**, DOI: 10.1371/journal.pone.0070881.
(11) Brown, D. R.; Schmidt, B.; Kretzschmar, H. A. *Nature* **1996**, *380*, 345−347.
(12) Selvaggini, C.; Gioia, L. D.; Cantù, L.; Ghibaudi, E.; Diomede, L.; Passerini, F.; Forloni, G.; Bugiani, O.; Tagliavini, F.; Salmona, M. *Biochem. Biophys. Res. Commun.* **1993**, *194*, 1360−1380.
(13) Singh, N.; Gu, Y.; Bose, S.; Kalepu, S.; Mishra, R. S.; Verghese, S. *Front. Biosci.* **2002**, *7*, 60−71.
(14) Brown, D. R. *Biochem. J.* **2000**, *352*, 511−518.
(15) Pillot, T.; Lins, L.; Goethals, M.; Vanloo, B.; Baert, J.; Vandekerckhove, J.; Rosseneu, M.; Brasseur, R. *J. Mol. Biol.* **1997**, *274*, 381−393.
(16) Ottaviani, M. F.; Mazzeo, R.; Cangiotti, M.; Fiorani, L.; Majoral, J. P.; Caminade, A. M.; Pedziwiatr, E.; Bryszewska, M.; Klajnert, B. *Biomacromolecules* **2010**, *11*, 3014−3021.
(17) Pillot, T.; Drouet, B.; Pinçon-Raymond, M.; Vandekerckhove, J.; Rosseneu, M.; Chambaz, J. *J. Neurochem.* **2000**, *75*, 2298−2308.
(18) Sonkina, S.; Tukhfatullina, I. I.; Benseny-Cases, N.; Ionov, M.; Bryszewska, M.; Salakhutdinova, B. A.; Cladera, J. *J. Pept. Sci.* **2010**, *16*, 342−348.
(19) Ragg, E.; Tagliavini, F.; Malesani, P.; Monticelli, L.; Bugiani, O.; Forloni, G.; Salmona, M. *Eur. J. Biochem.* **1999**, *266*, 1192−1201.
(20) Bergström, A. L.; Chabry, J.; Bastholm, L.; Heegaard, P. M. H. *Biochim. Biophys. Acta* **2007**, *1774*, 1118−1127.
(21) Grabenauer, M.; Wu, C.; Soto, P.; Shea, J. E.; Bowers, M. T. *J. Am. Chem. Soc.* **2010**, *132*, 532−539.
(22) Marcotte, E. M.; Eisenberg, D. *Biochemistry* **1999**, *38*, 667−676.
(23) Zou, W. Q.; Langeveld, J.; Xiao, X.; Chen, S.; McGeer, P. L.; Yuan, J.; Payne, M. C.; Kang, H. E.; McGeehan, J.; Sy, M. S.; Greenspan, N. S.; Kaplan, D.; Wang, G. X.; Parchi, P.; Hoover, E.; Kneale, G.; Telling, G.; Surewicz, W. K.; Kong, Q.; Guo, J. P. *J. Biol. Chem.* **2010**, *285*, 13874−13884.
(24) Valensin, D.; Gajda, K.; Gralka, E.; Valensin, G.; Kamysz, W.; Kozlowski, H. *J. Inorg. Biochem.* **2010**, *104*, 71−78.
(25) Kanapathipillai, M.; Ku, S. H.; Girigoswami, K.; Park, C. B. *Biochem. Biophys. Res. Commun.* **2008**, *365*, 808−813.
(26) Cosentino, U.; Pitea, D.; Moro, G.; Saracino, G. A. A.; Caria, P.; Varì, R. M.; Colombo, L.; Forloni, G.; Tagliavini, F.; Salmona, M. *J. Mol. Model.* **2008**, *14*, 987−994.
(27) Kawahara, M.; Koyama, H.; Nagata, T.; Sadakane, Y. *Metallomics* **2011**, *3*, 726−734.
(28) Gaggelli, E.; Bernardi, F.; Molteni, E.; Pogni, R.; Valensin, D.; Valensin, G.; Remelli, M.; Luczkowski, M.; Kozlowski, H. *J. Am. Chem. Soc.* **2005**, *127*, 996−1006.
(29) Jobling, M. F.; Huang, X.; Stewart, L. R.; Barnham, K. J.; Curtain, C.; Volitakis, I.; Perugini, M.; White, A. R.; Cherny, R. A.; Masters, C. L.; Barrow, C. J.; Collins, S. J.; Bush, A. I.; Cappai, R. *Biochemistry* **2001**, *40*, 8073−8084.
(30) Valensin, D.; Gajda, K.; Gralka, E.; Valensin, G.; Kamysz, W.; Kozlowski, H. *J. Inorg. Biochem.* **2010**, *104*, 71−78.
(31) Rivillas-Acevedo, L.; Grande-Aztatzi, R.; Lomelí, I.; Garcaí, J. E.; Barrios, E.; Teloxa, S.; Vela, A.; Quintanar, L. *Inorg. Chem.* **2011**, *50*, 1956−1972.
(32) Wang, Y.; Xu, J.; Wang, L.; Zhang, B.; Du, W. *Chem. Eur. J.* **2010**, *16*, 13339−13342.
(33) Wang, Y.; Feng, L.; Zhang, B.; Wang, X.; Huang, C.; Li, Y.; Du, W. *Inorg. Chem.* **2011**, *50*, 4340−4348.
(34) Wang, X.; Zhang, B.; Zhao, C.; Wang, Y.; He, L.; Cui, M.; Zhu, X.; Du, W. *J. Inorg. Biochem.* **2013**, *128*, 1−10.
(35) Wang, X.; He, L.; Zhao, C.; Du, W.; Lin, J. *J. Biol. Inorg. Chem.* **2013**, *18*, 767−778.
(36) Barnham, K. J.; Kenche, V. B.; Ciccotosto, G. D.; Smith, D. P.; Tew, D. J.; Liu, X.; Perez, K.; Cranston, G. A.; Johanssen, T. J.; Volitakis, I.; Bush, A. I.; Masters, C. L.; White, A. R.; Smith, J. P.; Cherny, R. A.; Cappai, R. *Proc. Natl. Acad. Sci. U.S.A.* **2008**, *105*, 6813−6818.
(37) Ma, G.; Huang, F.; Pu, X.; Jia, L.; Jiang, T.; Li, L.; Liu, Y. *Chem. Eur. J.* **2011**, *17*, 11657−11666.
(38) van Rijt, S. H.; Sadler, P. J. *Drug Discovery Today* **2009**, *13*, 1089−1097.
(39) Oguri, S.; Sakakibara, T.; Mase, H.; Shimizu, T.; Ishikawa, K.; Kimura, K.; Smyth, R. D. *J. Clin. Pharmacol.* **1988**, *28*, 208−215.
(40) Di Pasqua, A. J.; Goodisman, J.; Dabrowiak, J. C. *Inorg. Chim. Acta* **2012**, *389*, 29−35.
(41) Casini, A.; Reedijk, J. *Chem. Sci.* **2012**, *3*, 3135−3144.
(42) Xie, R.; Johnson, W.; Rodriguez, L.; Gounder, M.; Hall, G. S.; Buckley, B. *Anal. Bioanal. Chem.* **2007**, *387*, 2815−2822.
(43) Neault, J. F.; Tajmir-Riahi, H. A. *Biochim. Biophys. Acta* **1998**, *1384*, 153−159.
(44) Ivanov, A. I.; Christodoulou, J.; Parkinson, J. A.; Barnham, K. J.; Tucker, A.; Woodrowi, J.; Sadler, P. J. *J. Biol. Chem.* **1998**, *273*, 14721−14730.
(45) Tanley, S. W. M.; Schreurs, A. M. M.; Kroon-Batenburg, L. M. J.; Helliwell, J. R. *Acta Crystallogr., Sect. F: Struct. Biol. Cryst. Commun.* **2012**, *68*, 1300−1306.
(46) Calderone, V.; Casini, A.; Mangani, S.; Messori, L.; Orioli, P. L. *Angew. Chem., Int. Ed.* **2006**, *45*, 1267−1269.
(47) Tanley, S. W. M.; Schreurs, A. M. M.; Kroon-Batenburg, L. M. J.; Meredith, J.; Prendergast, R.; Walsh, D.; Bryant, P.; Levyc, C.; Helliwell, J. R. *Acta Crystallogr., Sect. D: Biol. Crystallogr.* **2012**, *68*, 601−612.
(48) Helliwell, J. R.; Tanley, S. W. M. *Acta Crystallogr., Sect. D: Biol. Crystallogr.* **2013**, *69*, 121−125.
(49) Wang, X.; Guo, Z. *Chem. Soc. Rev.* **2013**, *42*, 202−224.
(50) Egan, T. J.; Koch, K. R.; Swan, P. L.; Clarkson, C.; Van Schalkwyk, D. A.; Smith, P. J. *J. Med. Chem.* **2004**, *47*, 2926−2934.
(51) VanScyoc, W. S.; Sorensen, B. R.; Rusinova, E.; Laws, W. R.; Ross, J. B. A.; Shea, M. A. *Biophys. J.* **2002**, *83*, 2767−2780.
(52) Ronga, L.; Langella, E.; Palladino, P.; Marasco, D.; Tizzano, B.; Saviano, M.; Pedone, C.; Improta, R.; Ruvo, M. *Proteins* **2007**, *66*, 707−715.
(53) Jiang, D.; Li, X.; Williams, R.; Patel, S.; Men, L.; Wang, Y.; Zhou, F. *Biochemistry* **2009**, *48*, 7939−7947.
(54) Perez-Pineiro, R.; Bjorndah, T. C.; Berjanskii, M. V.; Hau, D.; Li, L.; Huang, A.; Lee, R.; Gibbs, E.; Ladner, C.; Dong, Y. W.; Abera, A.; Cashman, N. R.; Wishart, D. S. *FEBS J.* **2011**, *278*, 4002−4014.
(55) Qin, K.; Coomaraswamy, J.; Mastrangelo, P.; Yang, Y.; Lugowski, S.; Petromilli, C.; Prusiner, S. B.; Fraser, P. E.; Goldberg, J. M.; Chakrabartty, A.; Westaway, D. *J. Biol. Chem.* **2003**, *278*, 8888−8896.
(56) Khurana, R.; Coleman, C.; Ionescu-Zanetti, C.; Carter, S. A.; Krishna, V.; Grover, R. K.; Roy, R.; Singh, S. *J. Struct. Biol.* **2005**, *151*, 229−238.
(57) Biancalana, M.; Koide, S. *Biochim. Biophys. Acta, Proteins Proteomics* **2010**, *1804*, 1405−1412.

(58) Betcher, D. L.; Burnham, N. J. *Pediatr. Oncol. Nurs.* **1988**, *5*, 29−30.
(59) Forloni, G.; Angeretti, N.; Chiesa, R.; Monzani, E.; Salmona, M.; Bugiani, O.; Tagliavini, F. *Nature* **1993**, *362*, 543−546.
(60) Dupiereux, I.; Zorzi, W.; Lins, L.; Brasseur, R.; Colson, P.; Heinen, E.; Elmoualij. *Biochem. Biophys. Res. Commun.* **2005**, *331*, 894−901.
(61) Fioriti, L.; Angeretti, N.; Colombo, L.; Luigi, A. D.; Colombo, A.; Manzoni, C.; Morbin, M.; Tagliavini, F.; Salmona, M.; Chiesa, R.; Forloni, G. *J. Neurosci.* **2007**, *27*, 1576−1583.
(62) Jeong, J. K.; Moon, M. H.; SEOL, J. W.; Seo, J. S.; Lee, Y. J.; Park, S. Y.. *Int. J. Mol. Med.* **2011**, *27*, 689−693.